Localised π-electron states in the optical absorption spectrum of tetrahedrally coordinated amorphous carbon

© *M.S. Chekulaev, S.G. Yastrebov*

Ioffe Institute,
194021 St. Petersburg, Russia
E-mail: mchs89@gmail.com

The paper presents result of *ab initio* methods exploiting to calculate the molar extinction spectrum of some model clusters, the molecular hybrid $C_{24}H_{30}$ included. Based on the comparison of the calculation with the experimental spectra of the main allotropic modifications of carbon, the absorption maximum with an energy of ~ 6 eV in the absorption spectrum of highly tetrahedral amorphous carbon (ta-C) attributed to the $\pi \to \pi^*$ optical transitions of electrons in a single aromatic ring. The edge sites of the ring covalently bonded with the sp^3-hybridised carbon atoms of the amorphous matrix. The manifestation of a shoulder in the spectrum of the imaginary part of the refractive index of a film of highly tetrahedral amorphous carbon (ta-C), 4.6 eV, is assigned to $\pi \to \pi^*$ optical transitions of clusters distorted with hybrid Stone–Wallace-like defect, also covalently bonded with the amorphous matrix.

Keywords: interaction of light with matter, new forms of carbon, tetrahedrally coordinated amorphous carbon, Stone–Wales defect.

1. Introduction

„The diamond-like" variety of amorphous carbon, obtained under laboratory conditions in the form of amorphous tetrahedrally coordinated carbon films with a high content of the sp^3-phase, has a number of properties typical of amorphous semiconductors, such as the presence of a band gap and the possibility of changing the type of conductivity under the influence of doping. Therefore, this material is usually referred to the group of amorphous semiconductors. In foreign literature, it is referred to as ta-C, where the letter t refers to the word tetrahedral, a letter to the word amorphous. This material is of interest to researchers due to the expansion of its application areas, for example, in the creation of wear- and chemically resistant coatings. These properties of the material are manifested due to the high content of tetrahedrally coordinated bonds between carbon atoms in it. Besides, sp^2-hybridized clusters (according to modern terminology —graphene fragments) and their networks can be contained in its matrix [1]. Therefore, due to weak overlap of optical transparency areas between high-tetrahedral matrix and fragments of sp^2-hybridized clusters (graphene fragments and their networks), this material is almost an ideal medium for their study by optical spectroscopy methods due to the general interest in new allotropic carbon modifications.

Therefore, in this study, an example of a typical spectrum of the imaginary part of the refraction index ta-C obtained in the paper [2] is given, as well as its interpretation.

Since, as will be shown below, the most intense absorption band ta-C (see [2]) practically coincides with the known

from astrophysical observations band with a maximum ~ 217.5 nm (~ 5.67 eV), the results of the analysis of the spectrum of localized states of π-electrons of the hybrid cluster $C_{24}H_{30}$, the calculated molar extinction spectrum of which lies within this band, will be used. Be reminded, that earlier in our studies [3–6], by means of *ab initio* methods we optimized the geometry and studied the absorption of electromagnetic radiation of visible and ultraviolet radiation by hybrid nanoclusters of various types, including those representing a graphene fragment located in the center with a small number of aromatic rings, surrounded by a diamondden fragment bounded with its side sites, the dangling bonds of which are passivated by hydrogen. In addition, using the example of the Stone−Wales (SW) [6] defect, the influence of the defect on the molar extinction spectrum of such a hybrid cluster was considered. Based on the calculations, it was concluded that a graphene fragment surrounded by an sp^3 matrix can be a candidate for the role of a light absorber in the interstellar medium, leading to the formation of an intense band of light absorption by the interstellar medium with a maximum of 217.5 nm (~ 5.7 eV). In this study, we will calculate a shortened structure containing such a defect and study its optical properties.

Since the simplest cluster, $C_{24}H_{30}$, which absorption spectrum is the closest to the experiment, has already been found and studied by us in the study [4] using the methods *ab initio*, we will take it as the basis for further analysis. In this study we will study the mechanism of bonding to the matrix by means of hybrid side sites and calculate the effect of such attachment on its optical properties for two limiting cases. The first case — when all side sites

are used for bonding, and the second — when only one is used. To demonstrate the possibility of addition to the matrix, the side sites protons are replaced by carbon, and the remaining dangling bonds are passivated by hydrogen. It will be shown, that as a result sp^3-bond simulating the addition of a cluster to the matrix is formed. In this case, the system of π electrons of the cluster graphene sp^2-fragment is localized inside the matrix, surrounded by sp^3-hybridized carbon. Thus, the conditions are created for the geometric confinement of π electrons in the matrix. The set of optical transitions between size quantization levels of an isolated graphene fragment is responsible for the spectrum of optical absorption of light by such localized π-electrons states.

2. Experimental procedure

To study the localized states of π-electrons using *ab initio* methods, two problems were solved. The first one — optimization of the geometry of the $C_{24}H_{30}$ cluster, which side site is replaced by carbon, and the dangling bonds are passivated by hydrogen. Thus, to find out the possibility of conjugation with the ta-C matrix, we will add an additional C−H-bond modeling the bonding with the matrix to the $C_{24}H_{30}$ cluster side site. The image of $C_{24}H_{30}$ cluster with an added C−H bond is shown in Fig. 1 after geometry optimization, where the added carbon atom is colored green, and hydrogen one — colored yellow.

In addition, the $C_{32}H_{38}$ cluster containing the hybrid SW defect will be studied. The image is shown in Fig. 2. The cluster fragment containing the SW defect is colored turquoise.

Thus, in the present study, a new, hybrid type of defect is introduced, as shown in Fig. 2. It was formed in the same way as the classical SW defect, except that after the addition of hydrogen to the side sites, part of the sp^2-bonds between atoms was transformed into sp^3.

Ab initio methods were used for calculations. Note that the selection of a basis and a method for a specific problem solved by *ab initio* methods seems to be a fairly common practice and requires the looking through a significant number of available combinations and combinations of methods and bases, as well as a comparison of the calculation results with the experiment for as close systems as possible. However, although such a procedure seems to be very useful, and therefore necessary to perform, it is at the same time expensive in terms of time spent by both the experimenter and the computer. Indeed, in addition to B3LYP, even within the framework of DFT (density functional theory), there are many methods: classical, hybrid, double hybrid, etc. Each of them has its own features. Therefore, in order to save resources, the researchers often use literature data that tell about the successful application of certain methods and bases to solve similar problems. The study [7] reported on the successful application of the B3LYP exchange-correlation
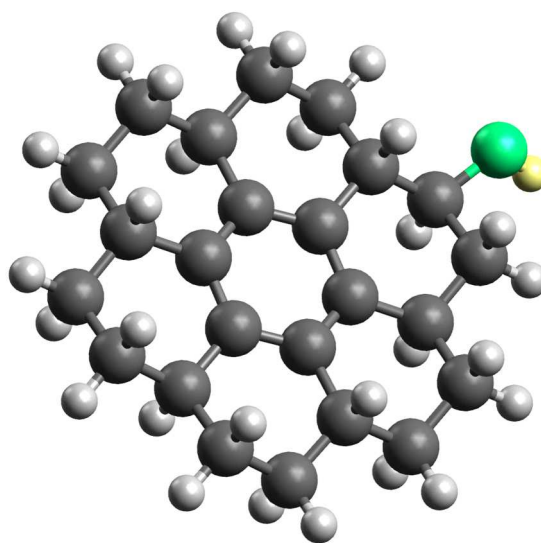
Figure 1. $C_{24}H_{30}$ cluster with the added CH-group. Carbon atoms are marked dark gray and green, hydrogen atoms — light gray and yellow. The total energy after geometry optimization is equal to -2536223 kJ/mol. (Colored figure version is given in the electronic version of the article).
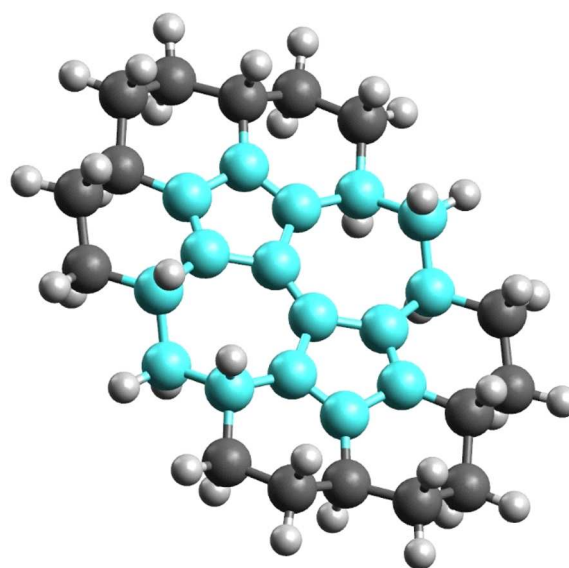
Figure 2. $C_{32}H_{38}$ cluster with a SW defect. Carbon atoms are marked dark gray and turquoise, hydrogen atoms — light gray. The total energy after geometry optimization is equal to -3242889 kJ/mol. (Colored figure version is given in the electronic version of the article).

hybrid functional with a small 3-21G$(^*)$ basis to optimize the geometry and simulate the spectral and electrochemical properties of complex carbon complexes. Therefore, in this study, to optimize the geometry of all the clusters under study and calculate their optical properties, we use the above mentioned exchange-correlation hybrid functional and basis, by analogy with the study [7].

For the calculations the GAUSSIAN 09 [8] package was used; in our case, the geometry optimization of the hybrid cluster was performed using the Bernie algorithm [9] together with the GEDIIS method (geometry optimization using energy-represented direct inversion in the iterative subspace) [10]. The calculation results are presented in Fig. 1, 2. The numerical values of total energy of the molecular hybrid achieved during optimization at the minimum point is given in the caption to Fig. 1, 2. The sign and order of magnitude of these energies correspond to the values obtained by applying a similar calculation method to known hydrocarbons (see, for example, [4]). After the geometry stability was confirmed the molar extinction spectrum was calculated using time-dependent method (in Russian literature — „non-stationary") of the density functional theory (time-dependent density functional theory, TD DFT). The set of basic functions described above was used for the calculation.

3. Results and discussion

The survey spectrum of optical absorption ta-C was taken from the study [2], and part of it, for the actual area, is shown in Fig. 3, 4 in comparison with the calculated data for different clusters considered in the study.

Four areas are distinguished on the spectrum. In the *1* area, the absorption increases with decreasing photon energy, in the infrared area. In the *2* area, at a photon energy somewhat higher than 4.2 eV, a shoulder is observed. With a further increase in energy in the *3* area, a maximum near 6 eV appears on the dependence, followed by a decrease with increasing energy > 6 eV. With a further increase in energy, the decrease is replaced by an increase in the area marked with *4* in the figure.

Since it goes about carbon, it is useful to compare it with the spectra of the main allotropic modifications — of diamond and graphite, the imaginary part of which is shown in Fig. 5. Note the growth of the imaginary part in the low-energy part of the spectrum, which repeats the trend for graphite. In gapless graphite this growth occurs partly due to optical transitions $\pi \to \pi^*$ and due to the presence of free electrons in the conduction band. We can also note the similarity in the area *2*, between the dependence for ta-C and graphite. If in the case of ta-C a shoulder was observed on the dependence, then for graphite — the maximum of the imaginary part. In the case of graphite, this maximum is formed by $\pi \to \pi^*$ transitions. Considering the similarity of both materials, we can attribute the presence of the ta-C spectrum shoulder to long graphene fragments embedded in an amorphous network of atoms linked by sp^3-hybridization. It is also possible that this network is connected with the inner and outer surfaces of the sample by analogy with the graphitized surface [111] of diamond [11]. The main difference between the spectra of graphite and diamond and ta-C, as can be seen from the figure, is the absorption band occupying the *3* area. Below, we will show that this
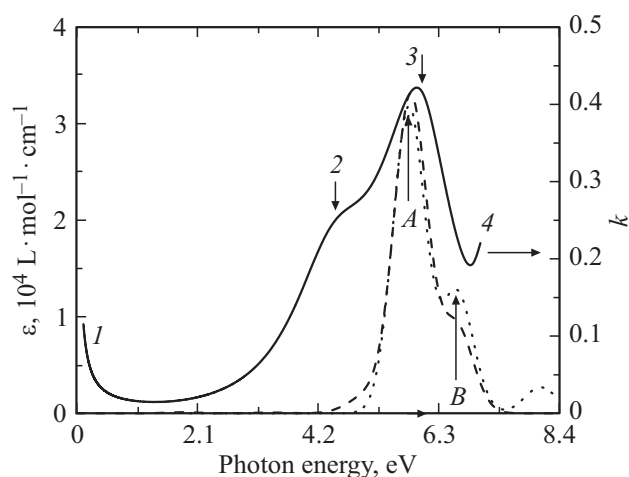
Figure 3. The calculated molar extinction spectrum for the c $C_{24}H_{30}$ fragment, — dotted line. The calculated molar extinction spectrum for a fragment with $C_{24}H_{30}$ and for a fragment with $C_{24}H_{30}$ with added C−H-group are shown by dotted and dashed lines respectively. The spectrum of the imaginary part of the refraction index ta-C [2] is shown as a solid line.
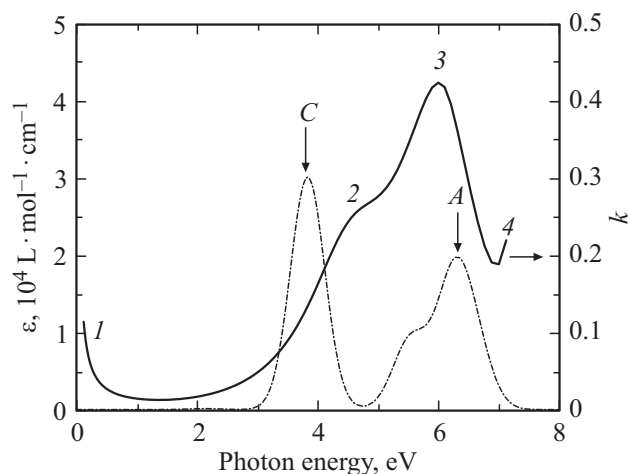
Figure 4. The calculated molar extinction spectrum for the fragment with the SW type defect — dash-and-dot line. The spectrum of the imaginary part of the refraction index ta-C [2] is shown as a solid line.

absorption band can also be attributed to optical transitions $\pi \to \pi^*$ of a graphene fragment, which electrons, due to the fragment small size, undergo geometric confinement.

For the perpendicular direction in the actual spectral range, the absorption is small compared to that shown in the figure.

Let us consider a hybrid cluster consisting of a single aromatic ring encapsulated by a diamondene fragment, as described above. The calculated molar extinction spectrum for such a cluster with the formula $C_{24}H_{30}$ is shown in Fig. 3. The absorption maxima in the actual spectrum regions are marked by vertical arrows and the letters *A* and *B*, as well as vertical arrows pointing upwards. Note
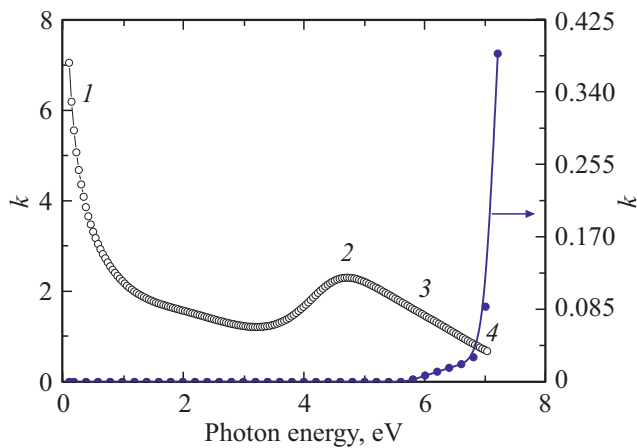
Figure 5. Solid circles — spectrum of the imaginary part of the diamond refraction index (experiment) [12]. Empty circles — spectrum of the imaginary part of the graphite refraction index (experiment) for the direction of the electric field of an electromagnetic wave parallel to the basal plane [13].

that the energy corresponding to the most intense maximum is ~ 5.9 eV, and the energy corresponding to the less intense maximum is ~ 6.7 eV. Such a graphene fragment containing one aromatic ring, bonded to the matrix by side sites, can exist in the ta-C variety under study. In this case the hydrogen of the edge cluster sites models its addition to the matrix atoms, predominantly bonded to each other by the sp^3- hybridization type. In this case, the manifestation of an intense absorption band in the ta-C spectrum, marked by the number *3*, can be due optical absorption of light π by the electron system of a single aromatic ring undergoing geometric confinement (optical transitions $\pi \to \pi^*$, where the letters π and π^* denote, respectively, localized states occupied by electrons and free from them).

To study the stability of the hybrid cluster when the side site hydrogen is replaced by carbon, the C−H group was added to it, as shown in Fig. 1. As the figure shows, the cluster remains stable. The corresponding calculation of the optical properties in comparison with the spectrum of the imaginary part of the refraction index ta-C is shown in Fig. 3. It can be seen that in the case of the hybrid cluster addition to the matrix through a single side site, the molar extinction spectrum is slightly modified.

It is also possible to find out the influence of the SW-type hybrid defect on the spectrum of localized states of π electrons. Similar calculations were made earlier [6], it was found that the SW defect leads to the formation of a specific feature in the shoulder region on the spectrum similar to that determined for ta-C. The molar extinction spectrum corresponding to the configuration of atoms stated above, shown in Fig. 2, is presented in Fig. 4. In comparison with the calculation results presented above, for a cluster distorted by a CW defect, the maximum of the *A* band shifts to higher energies area, 6.28 eV, accompanied by a decrease in its intensity. An absorption band 3.83 eV also appears,

which manifests itself in the spectrum shoulder region of the imaginary part of the refraction index ta-C (denoted in Fig. 4 by the letter *C*). The shoulder region, that appears in the t-aC spectrum is marked with a number *2* in Fig. 4, 5.

So, when comparing the calculations performed by the *ab initio* method, we managed to establish a relationship between the spectrum of the imaginary part ta-C and the calculated molar extinction coefficients of hybrid clusters of two types containing one aromatic ring, and a cluster containing the defect similar to a SW defect. All calculations reveal an absorption band with a maximum at the energy ~ 6 eV, that coincides with the most intense feature of the spectrum ta-C. The calculation for a cluster containing a defect similar to a SW defect allows to reveal an absorption band with a maximum of ~ 3.83 eV, located near the ta-C spectrum shoulder.

To explain the increase in absorption with decreasing photon energy in the spectrum IR region, we used above the similarity of this spectrum area with that measured for graphite and assumed that its nature is related to the formation of extended graphene fragments. To further study of this behavior of the imaginary part, we refine the model.

Above we compared the dimensionless imaginary part of the refraction index with the size spectrum of the molar extinction coefficient. The dimensional part, among other things, contains inverse centimeters, i.e., it is an analogue of the absorption coefficient α:

$$\alpha = \frac{4\pi k}{\lambda}. \qquad (1)$$

Only in this part of the article π it is a known mathematical constant, λ — electromagnetic radiation wavelength, k — imaginary part of the refraction index. The comparison of k and α is given in Fig.. 6.

It can be seen that, in addition to the absolute values of the quantities, the dependences in Fig. 6 differ only in the spectrum low-energy part, where α, in contrast to k, does not increase with decreasing energy. The positions of
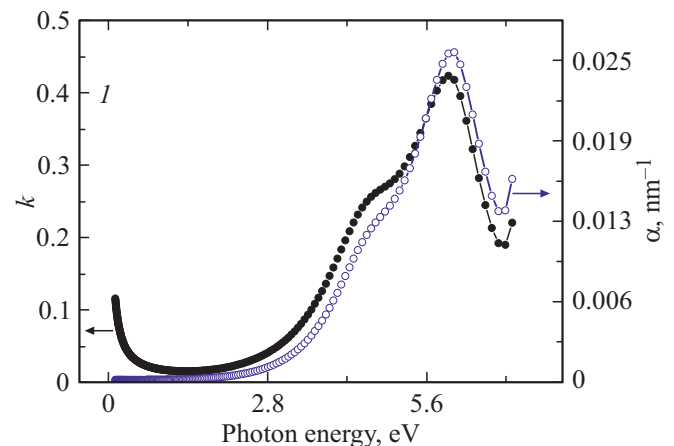
Figure 6. The comparison of the spectra of the imaginary part of the refraction index and the absorption coefficient ta-C.

the maxima and the shoulder on the α spectrum do not change. Therefore, the manifestation of a shoulder in the spectrum of the imaginary part of the film refraction index ta-C, 4.6 eV, can also be associated with the $\pi \rightarrow \pi^*$ optical transition in defective hybrid clusters covalently bonded to the amorphous matrix.

4. Conclusion

Using *ab initio* methods, the following was performed:

1) optimization of the geometry of hybrid clusters $C_{24}H_{30}$ with added CH-group and $C_{32}H_{38}$, distorted by the SW defect;

2) calculation of molar extinction spectra.

Based on the performed calculations, a conclusion was made about the stability of these clusters.

The comparison of the calculation with the experimental optical absorption spectrum ta-C made it possible to interpret the maximum with the energy ~ 6 eV, the contribution of optical transitions $\pi \rightarrow \pi^*$ of single aromatic rings covalently bonded to the amorphous matrix.

„The shoulder" on the spectrum in the ~ 4.6 eV region can also be attributed to the contribution of optical transitions $\pi \rightarrow \pi^*$ of hybrid clusters similar to $C_{32}H_{38}$, which are distorted by SW-type defects.

Conflict of interest

The authors declare that they have no conflict of interest.

References

[1] C.T. Toh, H. Zhang, J. Lin, A.S. Mayorov, Y. Wang, C.M. Orofeo, D.B. Ferry, H. Andersen, N. Kakenov, Z. Guo, I.H. Abidi, H. Sims, K. Suenaga, S.T. Pantelides, B. Özyilmaz. Nature, **577**, 199 (2020).
[2] J.I. Larruquert, L.V. Rodríguez-de Marcos, J.A. Méndez, P.J. Martin, A. Bendavid. Opt. Express, **21**, 27537 (2013). M.S. Chekulaev, S.G. Yastrebov. Pis'ma ZhTF, **45** (8), 47 (2019) (in Russian).
[4] M.S. Chekulaev, S.G. Yastrebov. Pisma ZhTF, **47** (19), 44 (2020) (in Russian).
[5] M.S. Chekulaev, S.G. Yastrebov. Pisma ZhTF, **47** (4), 19 (2021) (in Russian).
[6] M.S. Chekulaev, S.G. Yastrebov. Pisma ZhTF, **47** (24), 34 (2021) (in Russian).
[7] M.E. Zandler, F. D'Souza. Comptes Rendus Chimie, **9** (7–8), 960 (2006).
[8] M.J. Frisch, G.W. Trucks, H.B. Schlegel, G.E. Scuseria, M.A. Robb, J.R. Cheeseman, G. Scalmani, V. Barone, B. Mennucci, G.A. Petersson, H. Nakatsuji, M. Caricato, X. Li, H.P. Hratchian, A.F. Izmaylov, J. Bloino, G. Zheng, J.L. Sonnenberg, M. Hada, M. Ehara, K. Toyota, R. Fukuda, J. Hasegawa, M. Ishida, T. Nakajima, Y. Honda, O. Kitao, H. Nakai, T. Vreven, J.A.J. Montgomery, J.E. Peralta, F. Ogliaro, M. Bearpark, J.J. Heyd, E. Brothers, K.N. Kudin, V.N. Staroverov, R. Kobayashi, J. Normand, K. Raghavachari, A. Rendell, J.C. Burant, S.S. Iyengar, J. Tomasi, M. Cossi, N. Rega, J.M. Millam, M. Klene, J.E. Knox, J.B. Cross, V. Bakken, C. Adamo, J. Jaramillo, R. Gomperts, R.E. Stratmann, O. Yazyev, A.J. Austin, R. Cammi, C. Pomelli, J.W. Ochterski, R.L. Martin, K. Morokuma, V.G. Zakrzewski, G.A. Voth, P. Salvador, J.J. Dannenberg, S. Dapprich, A.D. Daniels, Ö. Farkas, J.B. Foresman, J.V. Ortiz, J. Cioslowski, D.J. Fox. Gaussian, **09**, (2013).
[9] H.B. Schlegel. Adv. Chem. Phys., **67**, 249 (2007).
[10] X. Li, M.J. Frisch. J. Chem. Theory Comput., **2**, 835 (2006).
[11] O.A. Shenderova, D.M. Gruen. *Ultrananocrystalline Diamond: Synthesis, Properties and Applications* (Oxford, Elsevier, 2012) chap. 7, p. 181.
[12] H.R. Philipp, E.A. Taft. Phys. Rev., **127**, 159 (1962).
[13] A.B. Djurišić, E.H. Li. J. Appl. Phys., **85**, 7404 (1999).